Organic Electronics 13 (2012) 1370–1376

Contents lists available at SciVerse ScienceDirect

Organic Electronics

journal homepage: www.elsevier.com/locate/orgel

Scaling behaviors of transient noise current in organic field-effect transistors

K.Y. Choo [a,b,*], S.V. Muniandy [a], C.L. Chua [a], K.L. Woon [a]

[a] Low-Dimensional Material Research Center, Department of Physics, Faculty of Science, University of Malaya, 50603 Kuala Lumpur, Malaysia
[b] Faculty of Engineering, Multimedia University, Jalan Multimedia, 63100 Cyberjaya, Selangor D.E., Malaysia

ARTICLE INFO

Article history:
Received 10 February 2012
Received in revised form 29 March 2012
Accepted 2 April 2012
Available online 20 April 2012

Keywords:
Detrended Fluctuation Analysis (DFA)
1/*f* noise
Brownian noise
Scaling behavior
Organic field-effect transistors (OFETs)

ABSTRACT

Top-contact and bottom-gate organic field-effect transistors (OFETs) based on poly(3-hexylthiophene), P3HT polymer has been fabricated with thermal treatment condition. Transient noise currents of the OFETs are measured at various source–drain voltages ranging from 0 V to −60 V with respect to a fixed gate voltage of −60 V. The results from conventional power spectral density method are compared with the more robust Detrended Fluctuation Analysis. The latter has been proven to be reliable for fractal signals particularly in the presence of nonstationary effects. Interesting transitions between multiscaling and monoscaling behaviors are observed in the power spectral density as well as the Detrended Fluctuation Analysis plots for different applied source–drain voltage V_{ds}. Uncorrelated white noise characteristics are observed for noise current measured at low V_{ds}, meanwhile 1/*f* noise-like scaling behaviors are observed at intermediate V_{ds}. At higher V_{ds}, the noise characteristics appeared to be close to Brownian-like power-law behavior. The scaling characteristics of the transient noise current can be related to the charge carrier dynamics. It is also found that large numbers of trap centers are induced when the device is stressed at high applied V_{ds}. The existence of these trap centers would disperse charge carriers, leading to 1/*f* type noise that could diminish the presence of Brownian noise in a very short time.

1. Introduction

The discovery of conducting polymer [1] has triggered huge interest for the development of organic and polymer based electronic and optoelectronic devices such as the organic field-effect transistors (OFETs), organic light emitting diodes (OLEDs), polymer solar cells, etc. [2,3]. For instance, field-effect transistors (FETs) [4–7] based on polymer and organic materials had been demonstrated since the early 80s. Since then, studies and development of OFET have become important in the viewpoint of technological prospects as well as the fundamental understanding from scientific aspects. This is mainly because OFET plays a significant role as the main component in cheap and flexible analog and digital electronics circuits. Moreover, OFET also serves as an important tool to study the carrier transport and light emission properties of organic semiconductors.

A field-effect transistor (FET) basically consists of an organic or inorganic semiconducting layer that is separated from the gate electrode by a layer of dielectric; source and drain electrodes that are separated by a (channel) length *L* and are in contact with the semiconducting layer. The source electrode is usually kept at zero bias and meant for charge carrier injection. When the gate voltage V_g (potential difference between the source and gate electrodes) is biased at a more positive (negative) level than that of the source voltage V_s, electrons (holes) are injected into the semiconducting layer within the channel region. The amount of accumulated charges is proportional to the gate

* Corresponding author at: Faculty of Engineering, Multimedia University, Jalan Multimedia, 63100 Cyberjaya, Selangor D.E., Malaysia. Tel.: +60 3 8312 5386; fax: +60 3 8318 3029.
E-mail address: kychoo@mmu.edu.my (K.Y. Choo).

1566-1199/$ - see front matter © 2012 Elsevier B.V. All rights reserved.
http://dx.doi.org/10.1016/j.orgel.2012.04.003

voltage V_g and the capacitance C_i of the dielectric. Before these charge carriers are moving to the drain electrode and then giving rise to current, the deep trap centers at the interface between the semiconducting and dielectric layers in the channel region have to be filled by these charge carriers first. Thus, there is an extra voltage, namely the threshold voltage V_{th}, required to compensate this effect and the effective gate voltage is given as V_g–V_{th} before current is resulted.

When a small source–drain voltage V_{ds} (potential difference between the source and the drain electrodes) is applied, charge carriers can flow through the channel region and be extracted from the drain electrode. The resulted current is linearly proportional to the source–drain voltage. If the V_{ds} is increased until $V_{ds} = V_g - V_{th}$, the FET is now at its pinch-off condition where a small depletion region is formed next to the drain electrode. Since the electric field in the depletion region is relatively higher than the electric field at the pinch-off point, thus space-charge saturation current is resulted when the charge carriers near the pinch-off point are swept across the depletion region into the drain electrode. If V_{ds} is continually increased, the depletion region will be expanded and leads to the shortening of the channel length. However, the potential at the pinch-off point still unchanged (V_g–V_{th}) and so for the potential that drops across the pinch-off point and the source electrode. Thus, the resulted current saturates after the pinch-off condition is achieved.

In organic field-effect transistors, the displacement of charge carrier is governed by the random hopping of charge carriers from one site to another empty site in which the hopping time typically follows a non-Gaussian distribution. The presence of trap centers due to both the structural imperfection and impurities significantly influence the displacement of the charge carriers and mobility. These trap centers need to be filled up first before net current flows and the filling of these trap centers by charge carriers depends on the gate voltage. Since current–voltage measurement can only represent the macroscopic behavior of the devices, it is not so useful for studying defects and trap centers related dynamics that are present in the devices. The gate voltage dependence of mobility obtained by using time-of-flight measurement can be used as a device parameter to probe the information of the structural imperfection and impurities [8]. However, high precision time-of-flight measurement requires an expensive and intricate setup.

Recently, many works have been carried out to study the performance of organic based devices [9–12] using low-frequency noise measurement. This approach has been proven to be useful for probing the transport dynamics at microscopic level, bulk or interface defects and traps. For instance, generation-recombination noise is associated with shallow trap levels occur in the device and $1/f$ noise is believed to be caused by a large number of generation-recombination trap centers that produces a cumulative generation-recombination noise [13]. These defects and trap centers could be induced during the fabrication processes of the devices. It is reckoned that accurate characterization of the low-frequency noise can serve as a simple and yet powerful device fabrication and performance diagnosis tool. Most conventional noise analyses use the power spectral density (PSD) method which is based on Fourier transform, and requires the noise to be stationary. However, noise often contains nonstationary effects and power-law scaling behavior as reported in [14–17]. The notion of nonstationary here refers is time-dependence of the basic statistics such as mean and variance of the time series; also the power spectral density. For example, the presence of trends or dynamical changes in the time series would render a simple power spectral density method to be inaccurate. A common practice would be to perform windowed Fourier transform or to perform the Fourier spectrum analysis on non-contagious segments of the time series and to take ensemble average of the power spectrum. This is done under presumption that the segments of the time series are approximated stationary. Hence, a more robust technique, Detrended Fluctuation Analysis (DFA) that can handle both stationary and nonstationary fractal time series (or noises) would provide better estimation of the scaling exponents and multiscaling regimes.

In this work, our aim is to characterize the scaling behaviors of noise currents and to link the noise characteristics to transport dynamics of organic field-effect transistors using power spectral density method and Detrended Fluctuation Analysis. Therefore, we first fabricated organic field-effect transistors using P3HT as the active material and measured the transient noise current of the devices. The measured transient noise currents were then characterized using power spectral density method and Detrended Fluctuation Analysis. Lastly, scaling behaviors of noise currents were used to explain the underlying transport dynamics of charge carriers in the presence of trap centers and applied source–drain voltage.

2. Device fabrication and measurement

A 100 nm thick silicon dioxide (SiO_2) layer is grown on top of an n-type silicon substrate to serve as the dielectric layer as shown in Fig. 1. The active layer of the device is made of Poly(3-hexylthiophene), P3HT is dissolved in chloroform and is spin-coated on top of the dielectric layer. P3HT is chosen in this study simply due to its high charge carrier mobility and commercial availability. The P3HT active layer is thermally treated at 120 °C for 10 min. The source and drain electrodes are deposited with a 50 nm thick gold on top of the P3HT active layer. The channel width (arranged in interdigitated design) and length are 11.2 mm and 40 μm, respectively.

Two Keithley 236 source-measurement units (SMUs) are used to bias the device and measure the current resulted from the device, where one unit of the SMUs is used to establish the source–drain voltage V_{ds} and measure the drain current I_{ds} while another unit of SMU is used to supply the gate voltage V_g and measure the gate current I_g. In order to obtain the temporal evolution of (transient) currents, devices are repetitively biased using the sweep function of the SMU while the resulted currents are measured during a fast integration time of 416 μs. The measured currents in time domain are then stored in the buffer

(maximum of 1000 readings) of the SMUs before they are recorded in a desktop computer for subsequent noise analysis using the conventional power spectral density method and the more robust Detrended Fluctuation Analysis approach. Power spectral density of the transient current is numerically computed by taking the squared modulus of fast-Fourier transform (FFT) of the transient current. This can be effortlessly done with the FFT subroutine available in the MATLAB program.

3. Noise analysis methods

Noise analysis has been useful for studying fluctuation processes in electronic and optoelectronic devices [9–17] where the fluctuation processes were observed to inherent with the fractal power-law scaling or $1/f$ type behaviors. A concrete model of nonstationary fractal process with generalized power spectral density is the fractional Brownian motion, which is widely used in the modeling of anomalous diffusion. The fractional Brownian motion (fBm) is defined as [18],

$$B_H(t) = \frac{1}{\Gamma(H+1/2)}\left[\int_{-\infty}^{0}\left(|t-s|^{H-1/2} - |-s|^{H-1/2}\right)dB(s) + \int_0^t |t-s|^{H-1/2}dB(s)\right] \quad (1)$$

with self-similarity parameter, namely, Hurst exponent satisfying $0 < H < 1$ and $B(t)$ represents the Brownian motion that is following a Gaussian distribution. For a standard fBm, $B_H(t)$ has zero mean, $E[B_H(t)] = 0$, with covariance is given as

$$C_{B_H(t)}(t_1,t_2) = \frac{1}{2}\left(|t_1|^{2H} + |t_2|^{2H} - |t_1-t_2|^{2H}\right). \quad (2)$$

The variance of fBm takes the power-law form as $Var[B_H(t)] \sim t^{2H}$. The self-similarity of $B_H(t)$ and the stationarity of its increments ensures that the generalized power spectral density of fBm, $S(f)$, having the power-law form as $S(f) \sim f^{-\beta}$ where f denotes the frequency and β is the scaling exponent of the power spectral density which has the value ranging from $1 < \beta < 3$. For special case, the values of Hurst exponent for $1/f$ (flicker) noise and Brownian motion are 0 and 0.5, respectively.

3.1. Power spectra density

The low frequency noise analysis using power spectra density method is implemented by computing the squared modulus of Fourier transformed of the measured transient noise currents. If the time series exhibits power-law scaling the power spectra would follow $S(f) \sim f^{-\beta}$. Slope of the log–log plot of the power spectra density yields the scaling exponent β. One can link the scaling exponent β to the Hurst exponent H if the underlying transport mechanism is described by fractional Brownian motion. The scaling exponent β gives useful information of the transport dynamics of the charge carriers hopping in the organic or polymer material of OFETs and also information on trap centers and defects. The presence of trap centers and defects could induce generation-recombination noise and $1/f$ noise in the devices that sets a maximum limit on the performance of the devices [9–12]. The occurrence of $1/f$ noise in a device could be observed at the low frequency region of the noise current power spectra density in which the power spectral density is inversely proportional to the frequency. In addition, it has been demonstrated in [14–17] that the nonstationary effect is naturally present in the noise current despite of the influence of the finite sampling size effect on the time series. In [17], it has also been shown that the power spectrum of the noise current follows a fractal power-law scaling or $1/f$ type behavior in which the scaling exponent of the power spectrum varies in the range of $1 < \beta < 2$ [17]. This is associated to the density of trap centers and the probability distribution of release rates that varies slowly with frequency [14]. The relationship of the scaling exponent β and the Hurst exponent is given as $\beta = 2H + 1$. The noise current can also be classified as uncorrelated white noise when $\beta = 0$ ($H = -0.5$), $1/f$ noise ($H = 0$) and Brownian-type noise when $\beta = 2$ ($H = 0.5$).

3.2. Detrended Fluctuation Analysis

Detrended Fluctuation Analysis is a statistical method that has been developed to study the existence of short-range or long-range correlation of time series. This method has first been used to study DNA sequences [19] and progressively finds its applications in other time series analysis such as that of the electrocardiogram (ECG) analysis [20–22], electroencephalogram (EEG) analysis [23–25], weather forecast [26] and electrical noise study in semiconductor devices [27,28]. Detrended Fluctuation Analysis has been proven to be a robust technique in time series analysis due to the capability of detecting whether a trend is superimposed on a time series [29] and the capability of differentiating stationary and nonstationary properties inherent in a time series [30]. This method contains of a few important steps [19,20,25] as outlined in the following paragraphs. The time series $x(i)$ is first subtracted from the mean value $\langle x \rangle$ and then integrated as given by Eq. (3)

$$Y(j) = \sum_{i=1}^{j} x(i) - \langle x \rangle \quad (3)$$

The integrated time series $Y(j)$ is then divided into boxes of equal length n. The next step involves fitting a linear least-squares line in each box of length n in which it reflects the local trend in that box and its y-coordinate of the local trend is represented by $Y_{fit}(j)$. The integrated time series $Y(j)$ is then detrended via subtracting it from the local trend $Y_{fit}(j)$ of each box. The average fluctuation $F(n)$ or the root-mean square of the difference between $Y(j)$ and $Y_{fit}(j)$ is computed as

$$F(n) = \sqrt{\frac{1}{N}\sum_{j=1}^{N}[Y(j) - Y_{fit}(j)]^2} \quad (4)$$

where N is the length of the time series. The average fluctuation $F(n)$ is then re-calculated for all box sizes leading to the power-law behavior namely $F(n) \sim n^{\alpha}$ if $x(i)$ is a fractal noise. The slope of linear scaling regime of the log–log plot

of $F(n)$ versus n gives the scaling exponents α which can then be used to deduce the correlation behavior of fractal noises. One can link the scaling exponent α to the anomalous diffusion process such as the fractional Brownian motion where $\alpha = H + 1$. When $\alpha = 0.5$, the integrated time series is associated with random walk whose original time series does not present any correlation between two events. This is the standard characteristic of white noise. The time series is said to be persistent with long memory effect when $0.5 < \alpha < 1$. On the other hand, anti-persistent time series exhibits short memory effect and in this case, $0 < \alpha < 0.5$. If $\alpha = 1$ ($H = 0$), time series is identified as having the characteristic of $1/f$ noise. Finally, when $\alpha = 1.5$ ($H = 0.5$), the integrated time series is considered as a Brownian-type noise.

4. Results and discussion

The output characteristic of the P3HT OFET is depicted in Fig. 2, where solid lines represent the sweeping of source–drain voltage from 0 V to −60 V at various gate voltages ranging from 0 V to −60 V. For all the applied gate voltages, it is clearly seen that the drain currents begin to saturate when the source–drain voltage V_{ds} is swept till close to the applied gate voltage and then saturated if V_{ds} is further increased. This is simply due to the pinch-off condition is already achieved.

The measured noise currents of OFETs at various source–drain voltage V_{ds} ranging from −1 V to −50 V while having the gate voltage V_g fixed at −60 V are shown in Fig. 3(a)–(e). It can be clearly seen that the profile of the noise current is gradually changing from white noise to $1/f$ noise and then to Brownian noise behavior as V_{ds} increases. The deviation of behavior of the transient noise current at difference V_{ds} is also observable through the calculated transient noise current power spectral density obtained at high frequency region in which the scaling exponent β of PSD is ranging from around 0.1 (white noise) to 2.0 (Brownian noise) as shown in Fig. 4(a)–(e). This observation is further evidenced by the DFA in which the calculated scaling exponent α of DFA obtained at short time window is changing from around 0.5 (white noise) to 1.50 (Brownian noise) as shown in Fig. 5(a)–(e).

At $V_{ds} = -1$ V, $1/f$ noise and shot noise are observed respectively at low and high frequency regions of PSD as shown in Fig. 4(a). The presence of $1/f$ noise at low frequency region of PSD is due to the summation of the generation-recombination noise spectral [13]. Generation-recombination noise is due to the random capturing and releasing of charge carries at trap centers. This also leads to the fluctuation of the number of free charge carriers occurring in the device. When the device is operated at low voltage (below −2.5 V), free charge carries are injected from the source contact, undergo trapping at and being released from the trap centers as they drift across the channel region of the OFET. Hence, each charge carrier arrives at the drain contact at a purely uncorrelated time. This transport mechanism causes the occurrence of shot noise in the device. The calculated scaling exponent α of DFA confirmed that the measured noise current at $V_{ds} = -1$ V is having the white noise behavior (Fig. 5(a)).

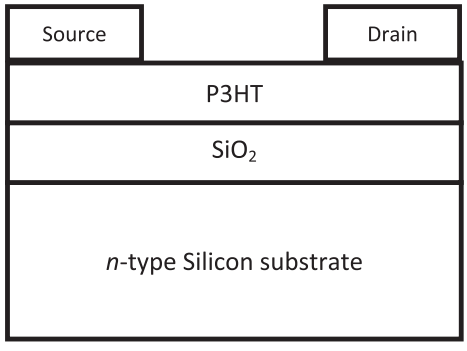

Fig. 1. Top-contact and bottom-gate OFET structure.

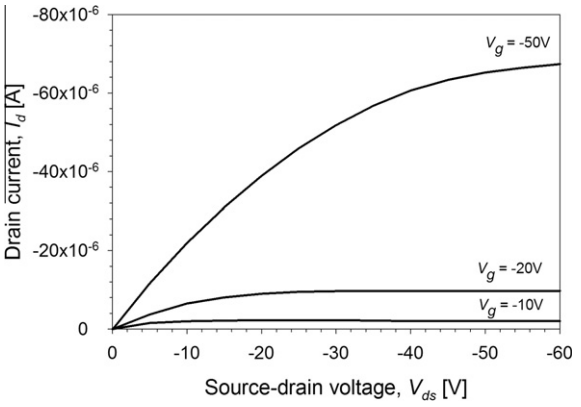

Fig. 2. Output characteristic of P3HT OFET with channel length of 40 μm. The source–drain voltage is swept from 0 V to −60 V for each gate voltage.

As V_{ds} increases to −10 V, both PSD method and DFA indicate that the noise current presents with $1/f$ noise at high frequency region of the PSD (Fig. 4(b)) and corresponds to short time window of DFA (Fig. 5(b)). On the other hand, Brownian noise is detected at low frequency region of the PSD and corresponds to large time window of DFA. It is also interesting to see that the white noise behavior of the noise current is detected by DFA using medium time window. When the device is biased at moderate V_{ds}, free charge carriers are injected from the source contact into the channel region, all trap centers will be immediately filled first while the remaining large amount of free charge carriers are continuously hopping towards the drain contact to produce current. Since electric field established at the channel region extends and covers relatively a larger area as compared to that of the low voltage, thus it contains a larger amount of trap centers that enhances the occurrence of generation-recombination noise. The summation of the generation-recombination noise spectral of a larger channel region eventually resulted in $1/f$ noise that happened at a very short time period [13]. After a very short time, all trap centers have been filled and the remaining free charge carriers are hopping towards the drain contact in which each hopping is not correlated with each other. Meanwhile, trapped charge carriers can be released from the trap centers and continue

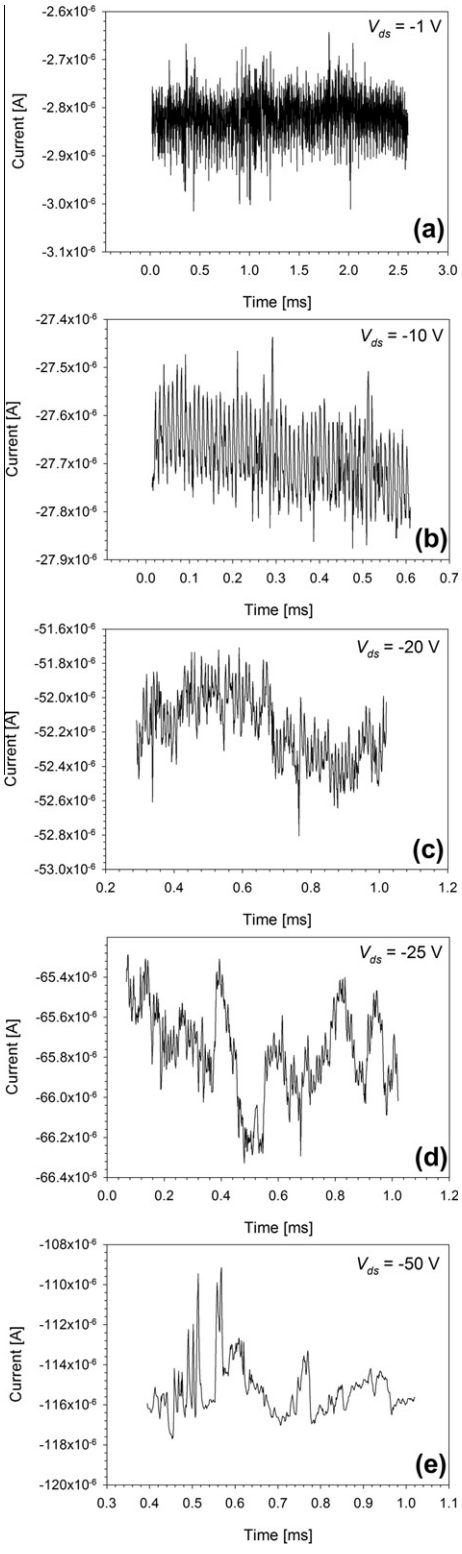

Fig. 3. Measured transient noise currents of OFETs at various V_{ds}: (a) −1 V, (b) −10 V, (c) −20 V, (d) −25 V and (e) −50 V.

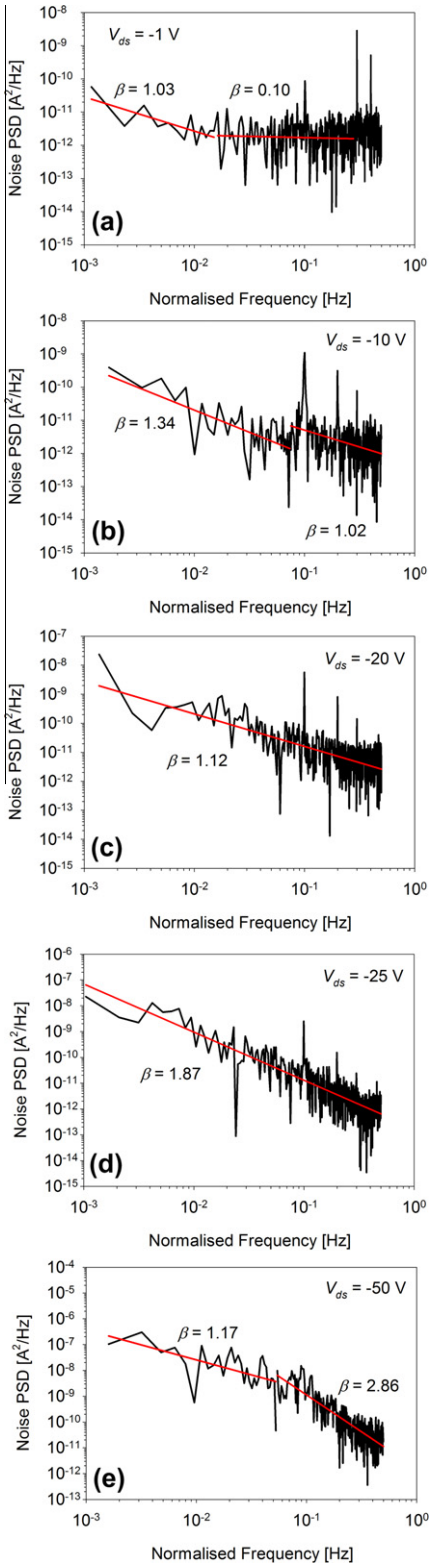

Fig. 4. Power spectral densities of transient noise currents of OFETs obtained at various V_{ds}: (a) −1 V, (b) −10 V, (c) −20 V, (d) −25 V and (e) −50 V. The straight line indicates the least-squares line of the PSD.

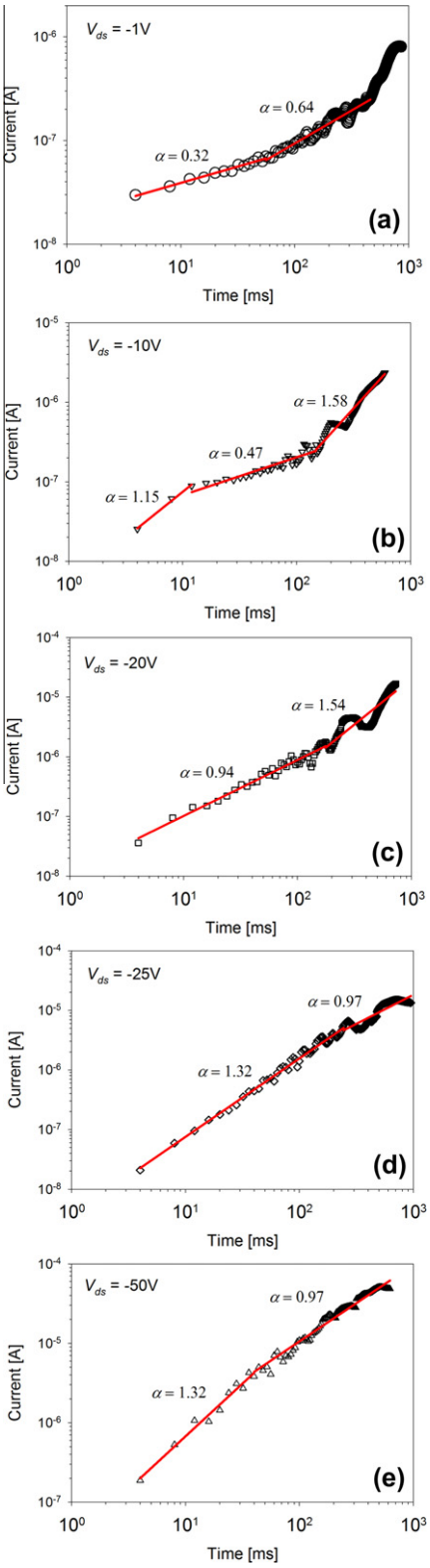

Fig. 5. Detrended Fluctuation Analysis of transient noise currents of OFETs obtained at various V_{ds}: (a) −1 V, (b) −10 V, (c) −20 V, (d) −25 V and (e) −50 V. The straight line indicates the least-squares line of the DFA.

to hop towards the drain contact. On the other hand, free charge carriers can be captured by trap centers again. Releasing of trapped charge carriers and re-trapping of free charge carriers are also occurring in an uncorrelated manner. Based on these reasons, the resulted current is fluctuating randomly like a white noise. In addition, Brownian noise-like current fluctuation is detected by both the PSD method and DFA (Fig. 5(b)). This could be attributed to the collective effect of hopping, capturing and releasing of charge carriers over a long time period.

At V_{ds} = −20 V, both PSD method and DFA indicate that the noise current presents with $1/f$ noise for the entire frequency region of the PSD (Fig. 4(c)) and at medium time window of DFA (Fig. 5(c)). This is simply due to the summation of generation-recombination noise spectra that lead to the $1/f$ noise when the electric field extended to cover a larger area of the channel region that contains a relatively huge amount of trap centers as compared to that of the number of trap centers at V_{ds} = −10 V. Besides that, Brownian noise is detected when the noise current is analyzed by DFA using large time window. This could be attributed to the collective effect of hopping, capturing and releasing of charge carriers over a long time period as observed at V_{ds} = −10 V. As shown in Fig. 3(c), it can be seen that the profile of noise current reveals a slight Brownian noise behavior that is detectable by DFA. This demonstrates that DFA is a more sensitive method as compared to PSD method to detect the non-stationary properties of the noise current.

At V_{ds} = −25 V, both PSD method and DFA indicate that the noise current presents with Brownian noise for the entire frequency region of the PSD (Fig. 4(d)) and at medium time window of DFA (Fig. 5(d)). It is interesting to see that charge carriers are now having an opposite transport dynamics as compared to the transport dynamics that occurred at lower V_{ds} (<−20 V). This suggests that correlation is induced between each charge carrier hopping and causes charge carriers hopping like Brownian particles in the device when the device is operated at high electric field. Besides that, $1/f$ noise is observed when the noise current is analyzed by DFA method using large time window in which PSD method is not sensitive enough to reveal this behavior. The occurrence of $1/f$ noise is simply due to the fact that a large amount of trap centers is provoked by the electrically induced stress on the active material which causes larger generation-recombination noises. The summation of generation-recombination noise spectra eventually yields the $1/f$ noise in the noise current that weakens the existence of Brownian noise.

Transport dynamics that happened at V_{ds} = −25 V is also reproducible when device was operated at even higher bias, V_{ds} = −50 V. The scaling exponent α of DFA indicates that charge carriers are hopping like Brownian particles. However, PSD method failed to analyze a highly non-stationary noise current since it calculated an unrealistic value of scaling exponent, $\beta > 2$ for Brownian noise. In addition, both PSD method and DFA indicate that the noise current presents with $1/f$ noise for the low frequency region of the PSD (Fig. 4(e)) and corresponds to large time window of DFA (Fig. 5(e)). Since the total number of trap centers occurred at −50 V is relatively larger than the total

number of trap centers at −25 V, thus the PSD method is able to sense the present of $1/f$ noise. The increment of the total number of trap centers when the device was operated at high applied voltage also signifies the degradation of the performance of device.

5. Conclusion

Noise currents of P3HT-based OFETs were measured at various source–drain voltages at a fixed gate voltage and analyzed using power spectral density method and Detrended Fluctuation Analysis. Detrended Fluctuation Analysis is found to be a more accurate and sensitive method to detect the change in the transport dynamics of charge carriers in which it is characterized by the scaling behavior of the noise current as compared to that of the power spectral density method. This is owing to the fact that power spectral density method becomes an unreliable tool when the noise current becomes a highly non-stationary time series. White noise is observed for the noise current measured at low V_{ds}, $1/f$ noise occurs at intermediate V_{ds}, and Brownian noise occurs at high V_{ds}. It is observed that a large number of trap centers was induced when the device was operated at high applied V_{ds} where these trap centers resulted in $1/f$ noise that could diminish the existence of Brownian noise in a very short time at high V_{ds}.

Acknowledgements

The authors would like to thank the Ministry of Higher Education (MOHE) of Malaysia for financial support through the Fundamental Research Grant Scheme (FRGS: FP003/2010B) and the University Malaya Research Grant (UMRG RG006/09AFR).

References

[1] J.L. Brédas, S.R. Marder, W.R. Salaneck, Macromolecules 35 (2002) 1137.
[2] J. Zaumseil, H. Sirringhaus, Chem. Rev. 107 (2007) 1296.
[3] M.P. Aldred, P. Vlachos, A.E.A. Contoret, S.R. Farrar, W. Chung-Tsoi, B. Mansoor, K.L. Woon, R. Hudson, S.M. Kelly, M. O' Neill, J. Mater. Chem. 15 (2005) 3208.
[4] F. Ebisawa, T. Kurokawa, S. Nara, J. Appl. Phys. 54 (1983) 3255.
[5] A. Tsumura, H. Koezuka, T. Ando, Appl. Phys. Lett. 49 (1986) 1210.
[6] A. Assadi, C. Svensson, M. Willander, O. Inganas, Appl. Phys. Lett. 53 (1988) 195.
[7] T. Mori, J. Phys.: Condens. Matter 20 (2008) 184010.
[8] C. Tanase, E.J. Meijer, P.W.M. Blom, D.M. de Leeuw, Phys. Rev. Lett. 91 (2003) 216601.
[9] O.D. Jurchescu, B.H. Hamadani, H.D. Xiong, S.K. Park, S. Subramanian, N.M. Zimmerman, J.E. Anthony, T.N. Jackson, D.J. Gundlach, Appl. Phys. Lett. 92 (2008) 132103.
[10] L. Ke, S. Dolmanan, L. Shen, C. Vijila, S.J. Chua, R.Q. Png, P.J. Chia, L.L. Chua, Peter, K.H. Ho, J. Appl. Phys. 104 (2008) 124502.
[11] L. Ke, X.Y. Zhao, R.S. Kumar, S.J. Chua, IEEE Electron Device Lett. 27 (2006) 555.
[12] Y. Xu, T. Minari, K. Tsukagoshi, R. Gwoziecki, R. Coppard, F. Balestra, J.A. Chroboczek, G. Ghibaudo, Appl. Phys. Lett. 97 (2010) 033503.
[13] S. Kasap, P. Capper, Springer Handbook of Electronic and Photonic Materials, Springer Science + Business Media Inc., Würzburg, 2006. p. 430.
[14] M. Nelkin, A.K. Harrison, Phys. Rev. B 26 (1982) 6696.
[15] J.J. Brophy, Phys. Rev. 166 (1968) 165.
[16] J.J. Brophy, J. Appl. Phys. 40 (1969) 3551.
[17] Z. Huo, L. Mao, M. Xu, C. Tan, Solid State Electron. 47 (2003) 1451.
[18] B.B. Mandelbrot, J.W.V. Ness, SIAM Rev. 10 (1968) 422.
[19] C.K. Peng, S.V. Buldyrev, S. Havlin, M. Simons, H.E. Stanley, A.L. Goldberger, Phys. Rev. E 49 (1994) 1685.
[20] C.K. Peng, S. Havlin, H.E. Stanley, A.L. Goldberger, Chaos 5 (1995) 82.
[21] H.V. Huikuri, J.S. Perkiömäki, R. Maestri, G.D. Pinna, Philos. Trans. R. Soc. A 367 (2009) 1223.
[22] M. Meyer, O. Stiedl, Eur. J. Appl. Physiol. 90 (2003) 305.
[23] J.M. Lee, D.J. Kim, I.Y. Kim, K.S. Park, S.I. Kim, Med. Eng. Phys. 26 (2004) 773.
[24] M. Ignaccolo, M. Latka, W. Jernajczyk, P. Grigolini, B.J. West, Phys. Rev. E 81 (2010) 031909.
[25] T. Penzel, J.W. Kantelhardt, L. Grote, J.H. Peter, A. Bunde, IEEE Trans. Biomed. Eng. 50 (2003) 1143.
[26] R. Matsushita, I. Gleria, A. Figueiredo, S.D. Silva, Phys. Lett. A 368 (2007) 173.
[27] M. Houssa, N. Vandewalle, T. Nigam, M. Ausloos, P.W. Mertens, M.M. Heyns, in: IEDM' 98 Technical Digest, 1998, p. 909.
[28] Y.H. Shiau, Solid State Commun. 151 (2011) 135.
[29] Z. Chen, P.Ch. Ivanov, K. Hu, H.E. Stanley, Phys. Rev. E 65 (2001) 011114.
[30] Z. Chen, P.Ch. Ivanov, K. Hu, H.E. Stanley, Phys. Rev. E 65 (2002) 041107.